

Electronic Supplementary Information

Electrical-field induced structural change and charge transfer of lanthanide-salophen based complexes assembled on Carbon Nanotube Field Effect Transistor devices

Gurvan Magadur,^{1,*} Fatima Bouanis,^{1,2} Evgeny Norman,² Régis Guillot,¹ Jean-Sébastien Lauret,³ Vincent Huc,¹ Costel-Sorin Cojocaru,² Talal Mallah^{1,*}

¹ Institut de Chimie Moléculaire et des Matériaux d'Orsay, Université de Paris Sud 11, CNRS, Bât. 420, 15 rue Georges Clemenceau, 91405 Orsay Cedex, France, ²Laboratoire de Physique des Interfaces et Couches Minces, Ecole Polytechnique, F-91128 Palaiseau, France, ³Laboratoire de Photonique Quantique et Moléculaire, 61, avenue du Président Wilson, 94230 Cachan, France

1. Materials and methods

All the reactants used for the synthesis of **1** and **2** were obtained from Aldrich. Deuterated solvents for NMR measurements were obtained from Cambridge Isotope Laboratories . HiPCo SWNT were obtained from Unidym™, Inc, CA, US. ¹H NMR spectra were recorded at 360MHz in CDCl₃. Elemental analysis were performed at Service de Microanalyses, ICSN-CNRS, Gif-sur-Yvette, France. Infrared spectra were recorded on a FT-IR spectrometer Perkin Elmer spectrum 100. Field effect transistors are homemade¹ and the electronic measurements were carried out on the semiconductor parametric analyzer Keithley 4200-SCS under ambient conditions. The photoluminescence excitation map was obtained by exciting the sample of SWNT with a Xe lamp coupled to a monochromator (Spectrapro 2150i, Roper Scientific) allowing an excitation wavelength between 350 nm and 800 nm.

2. Synthesis²⁻⁴

[Tb₂(salophen)₃] (**1**):

To a suspension of H₂salophen (disalicylidene-1,2-phenylenediamine) in ethanol (10 mL) under Ar was added Tb(NO₃)₃ (). The mixture was stirred at 80°C for 1 night under Ar. The yellow precipitate was collected by filtration, washed with cold ethanol and dried under vacuum to give **1**. A recrystallization of **1** was performed in a 8mL solution of tetrahydrofuran/ethanol (2:1). The mixture slowly evaporates to give pale yellow narrow needles and palettes. The resulting crystals were analyzed by X-ray crystallography giving the structure presented in 3.

¹H NMR (CDCl₃): δ (ppm) 6.0-6.6 (m), 6.7-7.5 (m), 8.01 (s), 8.46 (s). IR (KBr pellet) : v (cm⁻¹) 3450 (ν_{O-H}) 1608 (ν_{C=O}) 1534 and 1545 (ν_{C=C}) 1286, 1322 and 1345 (ν_{Ph-O}).

Cs[Tb(salophen)₂] (**2**):

2 was synthesized according to Chen and Archer.² C, H, N elemental analysis was conform to this previous work : C (51.64), H (2.30), N (5.96) Cs[Tb(salophen)₂]. 0.3 DMSO. Mass spectra: MS (ESI) : m/z (%) = 788.5 [M⁺](100).

3. X-ray measurements

X-ray diffraction data for Tb₂(salophen)₃ was collected by using a Kappa X8 APPEX II Bruker diffractometer with graphite-monochromated MoK radiation (= 0.71073 Å). Crystals were mounted on a CryoLoop (Hampton Research) with Paratone-N (Hampton Research) as cryoprotectant and then flashfrozen in a nitrogen-gas stream at 100 K. The temperature of the crystal was maintained at the selected value (100K) by means of a 700 series Cryostream cooling device to within an accuracy of ±1 K. The data were corrected for Lorentz polarization, and absorption effects. The structures were solved by direct methods

using SHELXS-97 and refined against F^2 by full-matrix least-squares techniques using SHELXL-97 with anisotropic displacement parameters for all non-hydrogen atoms.

Treatment on H: H atoms of the ligand were added from the difference Fourier map, and refined by the riding model. The H atoms of the water molecules were subsequently included in the refinement in geometrically idealized positions, with C—H = 0.96(3) Å H-H = 1.52(3) Å, and refined using the riding model with isotropic displacement parameters of Uiso(H) = 1.5Ueq (parent atom).

All calculations were performed by using the Crystal Structure crystallographic software package WINGX. The crystal data collection and refinement parameters are given in Table 1.

CCDC 883777 contains the supplementary crystallographic data for this paper. These data can be obtained free of charge from the Cambridge Crystallographic Data Centre via www.ccdc.cam.ac.uk/data_request/cif.

Ref :

[SHELXS-97] G. M. Sheldrick, SHELXS-97, *Program for Crystal Structure Solution, University of Göttingen, Göttingen, Germany* 1997.

[SHELXL-97] G. M. Sheldrick, SHELXL-97, *Program for the refinement of crystal structures from diffraction data, University of Göttingen, Göttingen, Germany* 1997.

[WINGX] L.J. Farrugia, *J. Appl. Cryst.* **1999**, 32, 837.

Compound	Tb (RX1066)
Formula	2(C ₆₂ H ₄₈ N ₆ O ₇ Tb ₂), H ₂ O
M _r	2631.87
Crystal size, mm ³	0.28 x 0.02 x 0.015
Crystal system	monoclinic
Space group	P 21/c
a, Å	22.027(3)
b, Å	23.021(3)
c, Å	22.557(2)
α, °	90
β, °	113.134(3)
γ, °	90
Cell volume, Å ³	10518(2)
Z	4
T, K	100(1)
F ₀₀₀	5224
μ, mm ⁻¹	2.731
θ range, °	1.01- 20.90
Reflection collected	76 551

Reflections unique	11062
R_{int}	0.1416
GOF	1.095
Refl. obs. ($>2\sigma(I)$)	7583
Parameters	706
wR ₂ (all data)	0.1832
R value ($>2\sigma(I)$)	0.0690
Largest diff. peak and hole (e \cdot Å $^{-3}$)	-2.001; 2.210

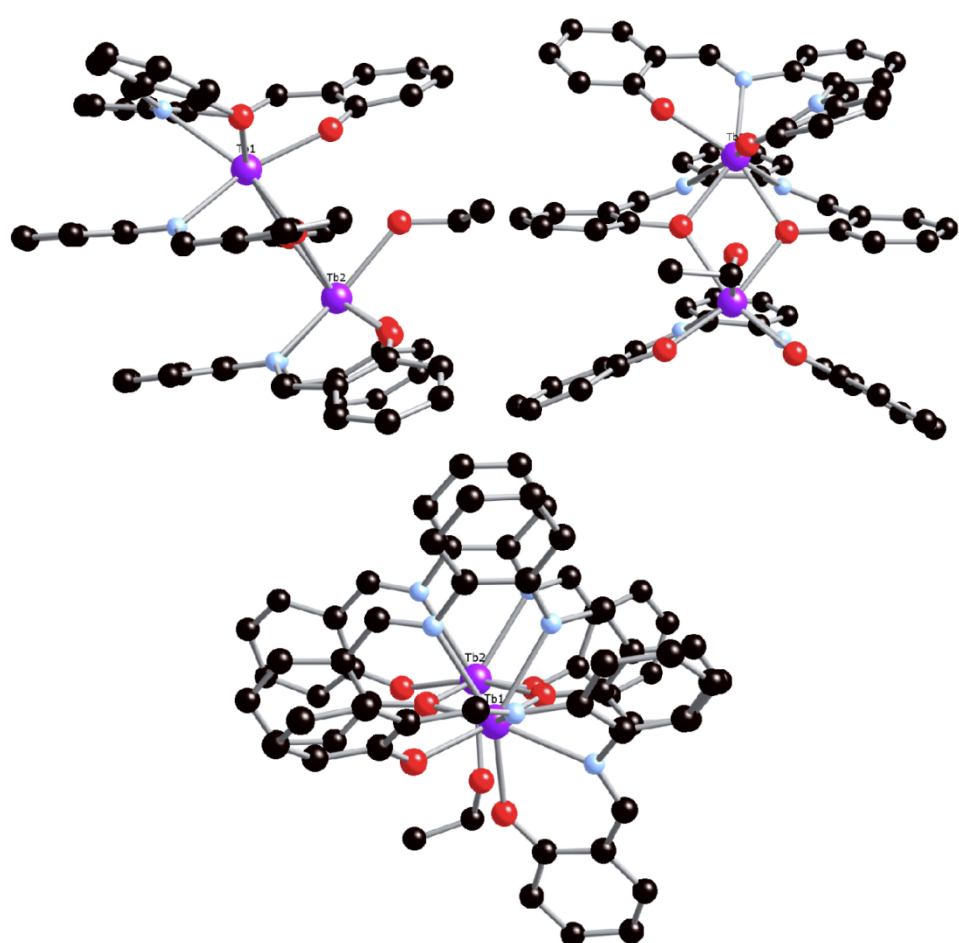


Figure S1. Different views of the structure of complex **1**.

4. UV-Vis and photoluminescence spectra

Spectroscopic Measurements:

Optical absorption spectra are recorded with a spectrophotometer (Lambda 900 Perkin–Elmer). A laser diode emitting at 532 nm is used as excitation source for photoluminescence experiments. The signal is dispersed in a spectrograph (Spectrapro 2300i, Roper Scientific) and detected by an IR CCD (OMA V, PI Acton). A UV/Vis Xe lamp and a monochromator (Spectrapro 2150i, Roper Scientific) are used as tunable light source for the photoluminescence excitation experiments.

UV-Vis spectra of 1:

The nanotube suspensions (HiPCO) are prepared according to Roquelet et al.⁵ by adding raw nanotubes at 0.15 mg.mL⁻¹ in a pH 8 Normadose buffer (10⁻² M, Prolabo) plus 2 wt% of sodium cholate (Sigma–Aldrich). The mixture is sonicated for 1.5h with an ultrasonic tip and ultracentrifuged at 120000 g for 1h. Then, the supernatant is drawn out. It consists in a suspension of isolated nanotubes. Nanotube functionalization is achieved by mixing the nanotube suspension with a solution of **1**(0,6 µmol) in DCM. After adding the complex solution to the nanotube suspension, the mixture is sonicated for 2 h with an ultrasonic tip. The sample is placed in a thermostat at 12°C during sonication. The phase corresponding to DCM evaporates slowly. The resulting suspension of SWNT/**1** is obtained and put to analysis.

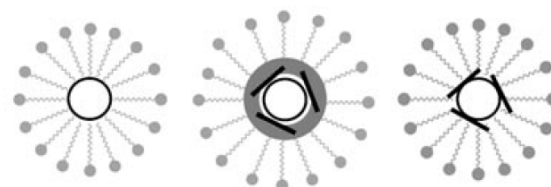


Figure S2. The nanotube is encapsulated in micelles. Some solvent molecules (DCM) are dragging **1** into the micelles. The volatile solvent evaporates, enabling the complexes to stack onto the SWNT wall.

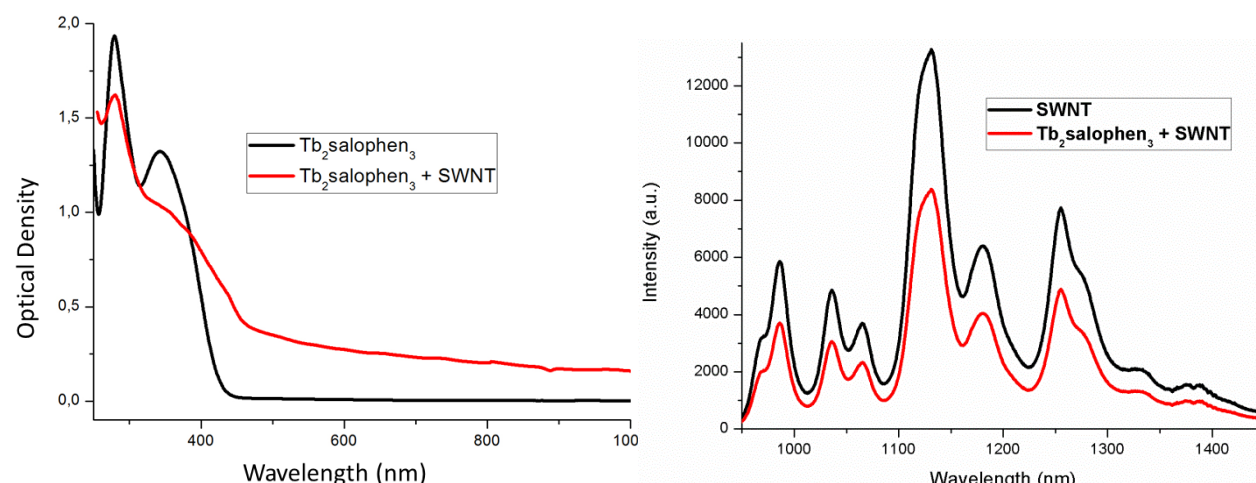


Figure S3. Left : UV-Visible spectra of **1** (black curve) and of **1** and SWNT in a pH 8 buffer with 2 wt% sodium cholate after evaporation of CH₂Cl₂ (red curve). Right : Photoluminescence spectra of SWNT in a pH 8 buffer with 2 wt% sodium cholate (black) and of **1** and SWNT in a pH 8 buffer with 2 wt% sodium cholate after evaporation of CH₂Cl₂ (red curve).

5. Fabrication of the FET devices and electrical measurements

The fabrication and basic electrical measurements were previously described by our group¹.

Here is a brief description:

SWNTs were grown by double hot filament assisted chemical vapor deposition (HFCVD) on 100 nm silicon oxide films on silicon substrates, using a new strategy for catalyst preparation based on Self Assembled Monolayer (SAM) which have been previously described. Random nanotubes networks, consisting of isolated carbon nanotubes, were obtained with excellent selectivity and high quality and uniformity. Their diameters varied from 1 to 2 nm. These networks were used for CNFETs device fabrication. Source-drain palladium contacts with a thickness of 40 nm were fabricated using standard UV lithography, e-beam evaporation and lift-off processes. It is generally accepted that Pd yields very good contacts for SWCNTs-metal contacts because of its high work function and corrosion resistance. The device geometry was varied with the source-drain channel length (L_{SD}) ranging from 2 to 20 μm and the channel width (W) ranging from 1 to 5mm were deposited to form an array of 4000 TFTs. Only the 2 μm and few of the 5 μm channel length devices were functional, suggesting that the CNTFET channel in this case consist of random but directly contacted isolated SWNT (little or no tube-tube percolation). The highly doped silicon substrate was used as common back-gate for all transistors. (Fig. S4). Finally, the metallic nanotubes were burned using the method proposed by IBM, semi-conducting SWNT being better suited for ultrasensitive detection (Fig. S5).

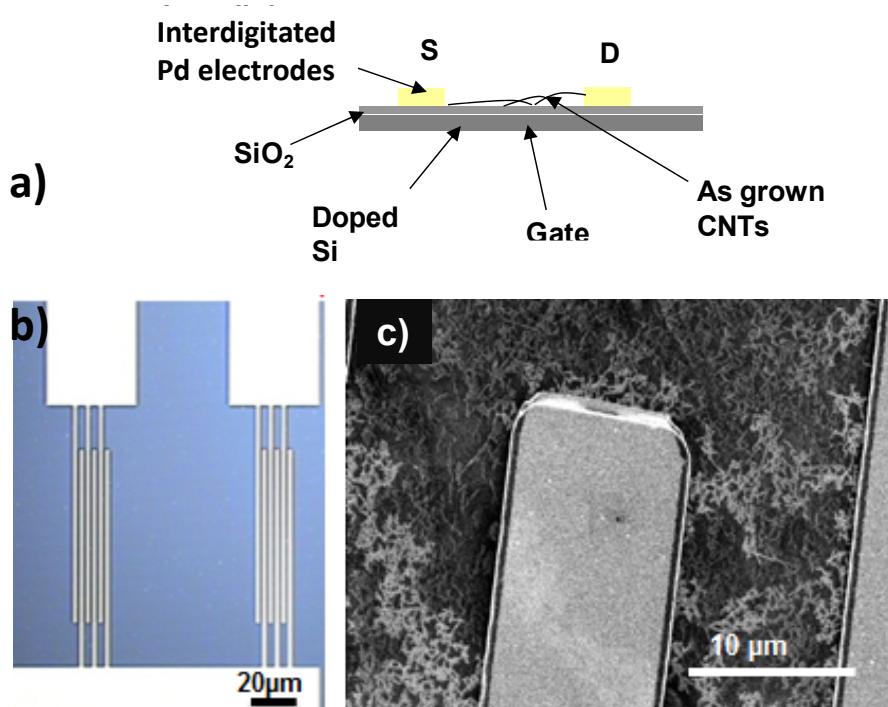


Figure S4. a) Schematic view of the SWNT-FET with a Si/SiO₂ (100 nm) back-gate. b) Photo of SWNT-FET , (c) Scanning electron microscope (SEM) image showing the gate region of a representative device consisting of a large number of SWNTs

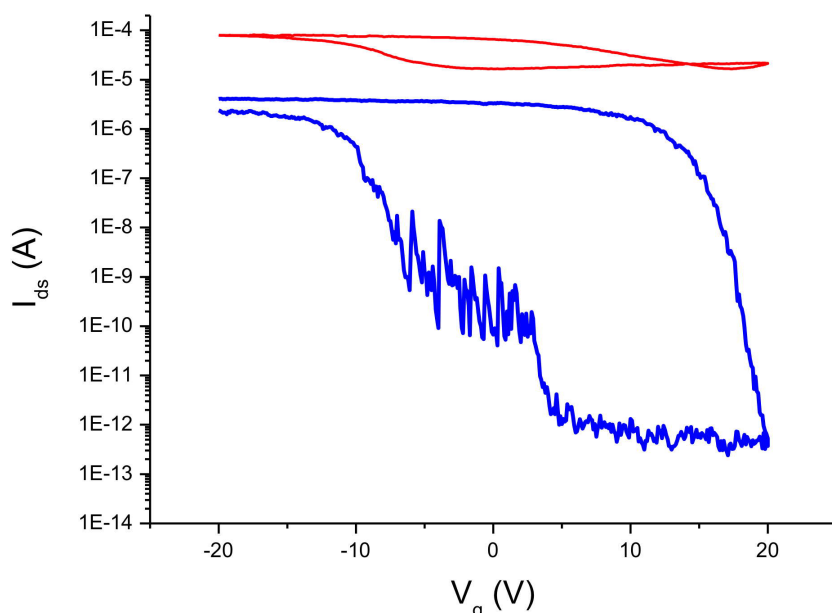


Figure S5 I_d vs. V_g curves for a CNFET device before (red curve) and after (blue curve) the burning process of the metallic SWNT.

All measurements here were realized with a 2V bias under air (1% humidity) and the gate was swept from -20 to +20V.

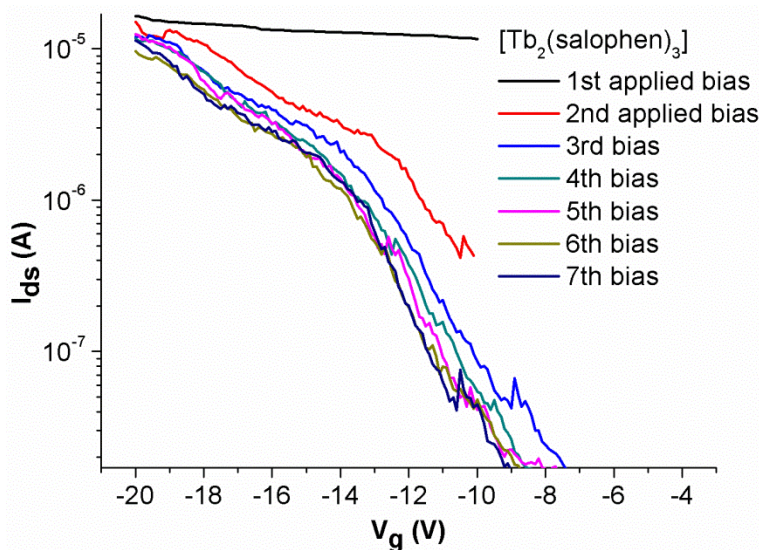


Figure S6 . I_{ds} vs V_g characteristics for a CNFET transistor modified with a layer of $[\text{Tb}_2(\text{salophen})_3]$. The bias is applied several successive times for V_g belonging to the [-20 V; -8 V] interval.

In order to prove the splitting in two parts of **1** is due to the application of a negative gate potential, several I_{ds} vs. V_g characteristics were obtained successively on the same transistor modified by the $[\text{Tb}_2(\text{salophen})_3]$ with a two minutes interval, using a 2 V bias for V_g varying from -20 V to -8V. During the first application of bias, the I_{ON} current is pretty high and slowly diminishes with the applied gate on the [-20 V; -8 V] interval, but as soon as a second bias is applied to the transistor, it drops significantly with V_g towards lower values. A stable characteristic is obtained for the system after the third measurement realized on the device. This proves that the drop of the current with V_g related to the splitting of the binuclear complex into two parts can be directly attributed to the important energy sent in the system with the application of the negative gate or to the electric field associated (Figure S6)

A global mechanism can be envisaged to explain the observations obtained for the CNFET devices (Fig. 4 in the main text). First, the $[\text{Tb}_2(\text{salophen})_3]$ is deposited as a randomly organized layer on top of the system.

Then, when a bias and a negative gate voltage are applied, the energy involved is sufficient to break two Tb-O bonds for complexes located near the SWNT, thus splitting the molecule into two charged fragments. Since one of them is negatively charged, most of those type of fragments assemble regularly on the SWNT surface. This phenomenon leads to an important charge transfer from the complexes to the nanotubes and to a small ambipolar effect. The other part of the initial complex attracted by the oppositely charged dielectric layer and interface can, since its terbium atom is relatively free, bond with some of the hydroxyl groups existing on the SiO₂ surface and constitute new charge traps which can annihilate the effect of the large initial [Tb₂(salophen)₃] screening layer. Away from the SWNT, the [Tb₂(salophen)₃] conserves its integrity.

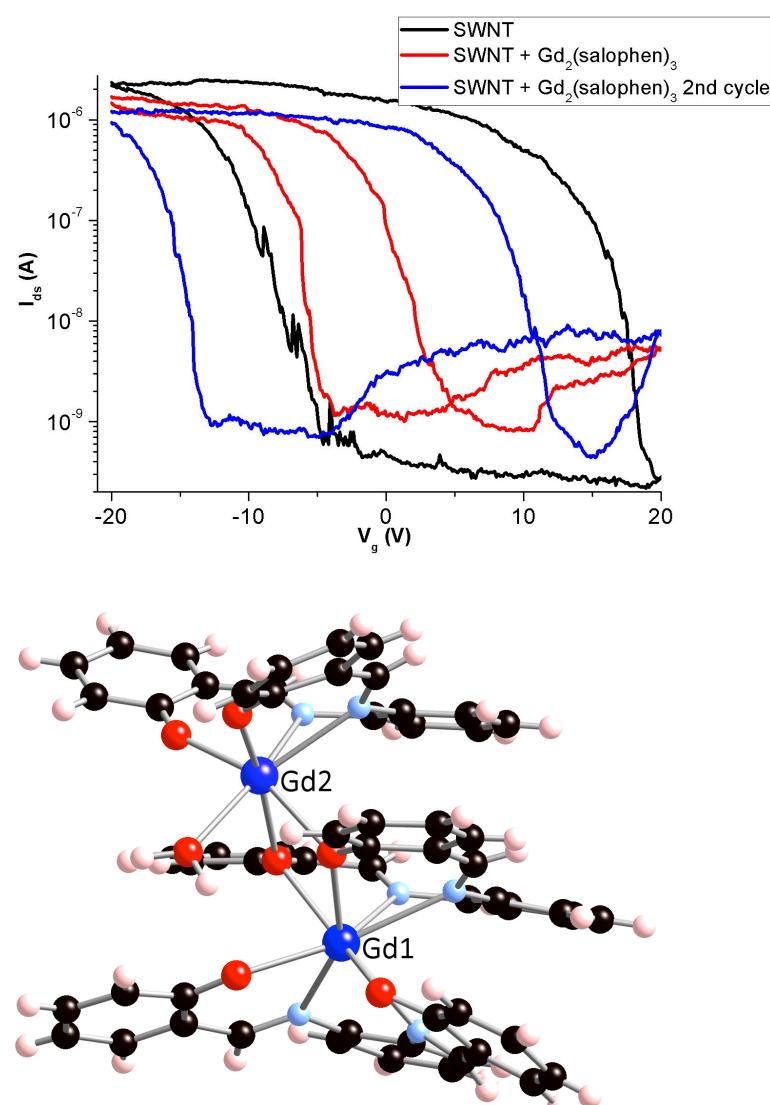


Figure S7. Transport characteristics of the Gd₂(salophen)₃ binuclear complex (top) and view of the crystal structure of the Gd₂(salophen)₃ complex (bottom).

1. G. Magadur, J-S. Lauret, G. Charron, F. Bouanis, E. Norman, V. Huc, C-S. Cojocaru, S. Gómez-Coca, E. Ruiz, and T. Mallah, *J Am Chem Soc*, 2012, **134**, 7896-7901.
2. H. Y. Chen and R. D. Archer, *Inorg Chem*, 1994, **33**, 5195-5202.
3. J. P. Costes, A. Dupuis and J. P. Laurent, *Inorg Chim Acta*, 1998, **268**, 125-130.
4. J. P. Costes, J. P. Laussac and F. Nicodeme, *J Chem Soc Dalton*, 2002, 2731-2736.
5. C. Roquelet, J. S. Lauret, V. Alain-Rizzo, C. Voisin, R. Fleurier, M. Delarue, D. Garrot, A. Loiseau, P. Roussignol, J. A. Delaire and E. Deleporte, *Chemphyschem*, 2010, **11**, 1667-1672.